ACS Photonics

pubs.acs.org/journal/apchd5

Article

Coupled Metamaterial–Phonon Terahertz Range Polaritons in a Topological Insulator

Sirak M. Mekonen, Deepti Jain, Seongshik Oh, and N. P. Armitage*

Cite This: ACS Photonics 2024, 11, 2242–2246

Read Online

ACCESS | Metrics & More | Article Recommendations | Supporting Information

ABSTRACT: We report terahertz time-domain spectroscopy experiments demonstrating strong light–matter coupling in a terahertz LC metamaterial (MM) in which the phonon resonance of a topological insulator thin film is coupled to the photonic modes of an array of electronic split ring resonators. As we tune the MM resonance frequency through the frequency of the low-frequency α mode of $(Bi_xSb_{1-x})_2Te_3$ (BST), we observe strong mixing and level repulsion between the phonon and MM resonance. This hybrid resonance is a phonon polariton. We observe a normalized coupling strength, $\eta = \Omega_R/\omega_c \approx 0.09$, using the measured vacuum Rabi frequency and cavity resonance. Our results demonstrate that one can tune the mechanical properties of these materials by changing their electromagnetic environment and therefore modify their magnetic and topological degrees of freedom via coupling to the lattice in this fashion.

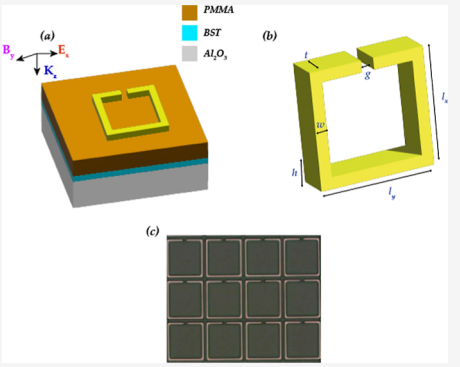

KEYWORDS: *phonon-polariton, metamaterials, topological insulator, strong-coupling, split-ring resonators, normal mode splitting, terahertz*

INTRODUCTION

Metamaterials (MMs) are artificial composite systems that offer exceptional control of electromagnetic properties due to the capability to engineer their electric and magnetic resonances by controlling the geometry and size of the individual subwavelength constituents. They offer the possibility to achieve strong coupling between highly confined electromagnetic fields and localized or propagating quasiparticles such as surface plasmon polaritons in metals and superconductors,[1] phonon polaritons in polar dielectrics,[2,3] and exciton polaritons in organic molecules and transition metal dichalcogenides.[4−6] Recently, MMs have been used to control the electron–phonon interaction of topological insulators (TIs) via their surface states.[7] TIs, a class of quantum materials with robust metallic surface states protected by the topological properties of the bulk wave functions,[8−11] have gathered a growing interest due to both their interesting fundamental physics and their potential applications in terahertz detectors[12] and spintronic devices.[13] These applications can potentially be realized through the polariton interaction, which arises from strong light–matter interactions between a confined electromagnetic field (or cavity resonance) and a matter excitation.

A strong light–matter interaction between lattice vibration and a confined electromagnetic field can reach the strong coupling regime, where coherent exchange of energy between light and matter becomes reversible. In this regime, coupled light–matter polaritons form hybrid states where they can coherently exchange energy at the characteristic rate of the vacuum Rabi frequency Ω_R, which is dominant with respect to other loss mechanisms in the system.[14,15] A polariton system based on novel functional materials could offer an efficient quantum level system with tunable sources and detectors, optical filters, and qubits operating in the far-infrared frequency range.[16−20] They may also afford the possibility of tuning the mechanical properties of materials (and, therefore, their electronic or magnetic properties through phonon coupling) by changing their electromagnetic environment. Phonon–polariton coupled systems with MMs in the mid-infrared range[2,21] have been shown in previous investigations as well as THz range surface plasmon polaritons.[22−24] In the most dramatic cases, it has been proposed that one can drive phase transitions in materials like $SrTiO_3$ via cavity coupling.[25] In this work, we present evidence of strong coupling between the α phonon mode in $(Bi_xSb_{1-x})_2Te_3$ (BST) thin films and the inductive–capacitive resonance of a split ring resonator (SRR) metasurface via the emergence of level repulsion. We performed time-domain terahertz spectroscopy (TDTS) on the resulting BST–SRR hybrid metasurfaces. The observed level repulsion results in the opening of a small transmission

Received: December 27, 2023
Revised: April 25, 2024
Accepted: April 26, 2024
Published: May 16, 2024

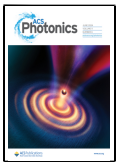

https://doi.org/10.1021/acsphotonics.3c01879
ACS Photonics 2024, 11, 2242–2246

window within the absorption band of the uncoupled phonon. We expect that the strength of the coupling can be altered through the design of the SRR. Mode assignments were aided through extensive simulations. In order to parametrically sweep the LC resonance frequency across the α mode, we fabricated multiple metasurfaces using standard photolithography techniques. Our measurements reveal level repulsion and hybridization of the coupled systems. This was evident by the formation of a large Rabi splitting with a normalized coupling strength $\eta \approx 0.09$. Our result is the first to show the control over the mechanical properties of TIs by tuning their electromagnetic environment in the terahertz (THz) frequency range.

MATERIALS AND METHODS

Figure 1a is a schematic of the unit cell of our BST film metasurface, which is composed of an array of SRRs deposited

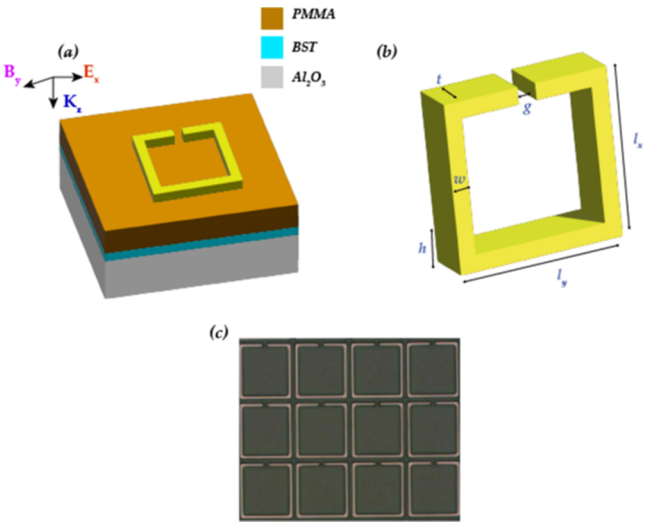

Figure 1. Design of multiscale TI metasurfaces. (a) Schematic of the unit cell showing a thin-film interface between the metallic SRR and Al_2O_3 substrate with the corresponding electromagnetic excitation configuration. (b) Side view schematic of the unit cell with the relevant periods p and resonator size l: $p_x = p_y = 44$ μm, $l = 34$ μm, $w = 3$ μm $g = 1.5$ μm, and $t = 100$ nm. (c) Optical microscopic image (20×) of a fabricated BST−SRR array.

on a TI film. The gap in SRRs serves as a capacitor, whereas the ring serves as an inductor giving an LC resonance. Generally, the resonance frequency of SRRs can be given as $f_0 \approx 1/(2\pi\sqrt{L_c C})$, where the inductance L_c and the capacitance C are determined by the SRR dimensions and the effective refractive index of the environment. At the LC resonance, the incident electric field induces a large accumulation of oscillating surface charges at the ends of the metal strips resulting in a strong electric field confinement in the capacitive gaps.[3,26−29] The resonance frequency of the SRR generally scales inversely with its dimension. We synthesized samples of $(Bi_xSb_{1-x})_2Te_3$ (BST) thin films with 20 quintuple layers on a 0.5 mm-thick sapphire (Al_2O_3) substrate by molecular beam epitaxy as discussed in ref 30. We performed finite element method (FEM)-based simulations (Ansoft HFSS) to identify the dimensions of SRRs with expected resonance frequencies ranging from 1.1 to 1.9 THz. Afterward, the desired metasurfaces were achieved by fabricating SRRs by using standard photolithography. We fabricated on top of a 1 μm poly(methyl methacrylate) layer on top of a Al_2O_3 substrate that allowed us—in addition to presumably tuning the coupling to the film—to strip off the SRR cleanly and redeposit another configuration of SRRs on top. The period $p_x = p_y$ and length $l_x = l_y$ of the SRRs were varied from 50 to 44 μm and 40 to 28 μm, respectively, while the width $w = 3$ μm and gap $g = 1.5$ μm were fixed. We used a TOPTICA (Teraflash) TDTS system to measure the THz transmission spectra of our samples. The incident THz pulse was polarized parallel to the x axis as shown in Figure 1a (see the Supporting Information). Figure 1c shows an image of one of the fabricated composite BST−SRR arrays that gives an SRR resonance frequency of 1.5 THz.

RESULTS AND DISCUSSION

In Figure 2a, we show the FEM simulation of a transmission spectrum for SRRs on an Al_2O_3 substrate. By tuning the lateral

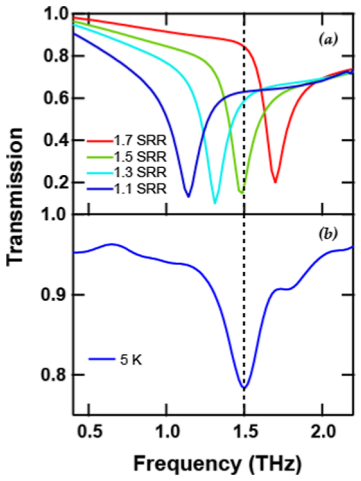

Figure 2. Numerical simulations of SRRs and TDTS data on Al_2O_3 at 5 K. (a) Simulated THz transmission spectra of SRR's at different resonance frequencies at different l. (b) TDTS transmission spectrum of the phonon resonance frequency of BST.

dimension l of the SRR, we expect to tune their resonant frequencies from 1.1 (4.55) to 1.7 (7.03) THz (meV). As the dimension of the SRRs decreased, the absorption exhibits a blue shift. Thus, it is possible to match the uncoupled resonant frequency of a SRR to the resonance of the material system. The 5 K transmission spectra of a bare BST film (with no SRR) is shown in Figure 2b. The absorption peak at ≈1.5 THz is the transverse optical α phonon mode that in the binary compounds Bi_2Se_3, Bi_2Te_3, Sb_2Te_3, and Sb_2Se_3 is attributed to an E_1^u mode that corresponds to the sliding motion of atomic layers past each other.[31] In the nonstochiometric compounds, phonons in this spectral range were found to extrapolate smoothly with atomic mass from Bi_2Te_3 to Sb_2Te_3 and from Bi_2Se_3 to In_2Te_3. This α mode has been investigated extensively in the context of THz studies of TIs.[10]

To sweep the SRR frequency across ω_{Ph}, we fabricated seven distinct SRRs on 20 nm-thick BST films (see the Supporting Information). At room temperature, the absorption of the SRRs predominates over the phonon mode absorption, primarily because the TI phonon modes become very broad due to scattering, resulting in overdamped absorption spectra. Consequently, we can accurately predict the frequencies of the

https://doi.org/10.1021/acsphotonics.3c01879
ACS Photonics 2024, 11, 2242−2246

SRRs decoupled from phonons, but when deposited on BST, phonons are heavily damped at elevated temperatures (see the Supporting Information). Therefore, we designate the different SRRs based on these predicted "bare frequencies".

At low temperatures, the behavior is very different. Here, the phonon resonance is strong, and when the SRR frequency is tuned to it, the effects of mixing and level repulsion are prominent. In Figure 3, we show the transmission data for the

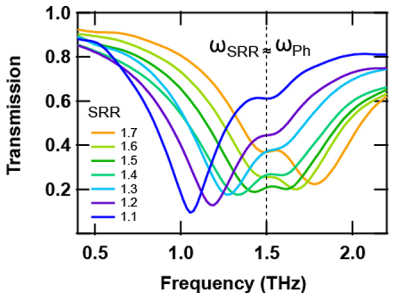

Figure 3. TDTS data on BST−SRR at 5 K (a) TDTS transmission spectrum of the seven SRR MM arrays deposited on the BST films.

BST−SRR hybrid systems at 5 K for ω_{SRR} ranging from 1.1 (4.55) to 1.7 (7.03) THz (meV). One can see two notable transmission dips for all samples that indicate two resonances. When their frequencies are far from each other, we can assign a clear local character. Judging from the data in Figure 2, the more prominent feature has largely SRR character and a higher Q-factor. We note though that as the SRR resonance is swept across ω_{Ph}, the two peaks always maintain a separation, and their intensities become similar. As the resonances are tuned through each other, the lower peak gets further damped and the upper peak sharpens, indicating that the local character of excitations changes as they are tuned through each other.

We fit the data of Figure 3 to a double-Lorentzian model to extract the eigenfrequencies ω_- and ω_+ and damping rates $\Gamma_\pm$ for all SRRs. Representative fits to these spectra can be found in the Supporting Information. Our BST−SRR hybrid system can be considered as two coupled oscillators, one of which has a fixed frequency (the BST phonon), where its electromagnetic environment is tuned by the SRR frequency. When both oscillators are similar in frequency, they form a coupled system, and an anticrossing is observed. This results in a periodic transfer of energy between the phonon and SRR through vacuum Rabi oscillations, which is proportional to the splitting at the anticrossing point.[32]

In Figure 4a, we plot the measured eigenfrequencies at 5 K versus the uncoupled resonance frequencies that we obtained at 297 K for the BST−SRR hybrid systems. The experimentally obtained peak positions, ω_+ and ω_-, are shown in circles. One can see a classic signature of level repulsion and mixing of two excitation branches with each other. As the uncoupled resonances approach each other, their distinct local characters are lost, and new coupled excitations are formed that are symmetric and antisymmetric combinations of the bare excitation. Our observation is evidence for the formation of a phonon−polariton hybrid from the coupling of the SRR resonance and α mode phonon.

The observed level repulsion behavior can be understood classically and be described using a coupled oscillators model[33]

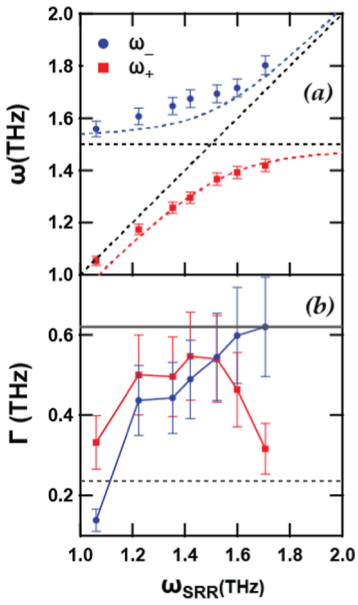

Figure 4. Dispersion and inverse lifetime of the coupled MM−phonon system. (a) Frequency of hybridized phonon modes of BST and the LC mode of SRRs. (b) Inverse lifetime of the resonances. Gray lines represent the estimation of the uncouple SRR decay rate and the phonon without SRR rates.

$$\omega_\pm^2 = \frac{1}{2}[\omega_{SRR}^2 + \omega_{Ph}^2 \pm \sqrt{(\omega_{SRR}^2 - \omega_{Ph}^2)^2 + \Omega_R^2 \omega_{SRR}\omega_{Ph}}] \quad (1)$$

We fit the observed level repulsion to eq 1 as indicated in Figure 4a to obtain the coupling parameters. The strength of the coupling, Ω_R, for when $\omega_{SRR} \approx \omega_{Ph}$, is found to be 0.27 (1.12) THz (meV). The observed splitting is a significant fraction of the α phonon mode resonance, which indicates a strong light−matter interaction at the avoided crossing. The normalized coupling strength ratio, $\eta = \frac{\Omega_R}{\omega_c}$, between the Rabi frequency and BST−SRR resonance frequency, is found to be $\eta \approx 0.09$.

It is also interesting to note the behavior of the peak widths as the bare SRR frequency is swept. Figure 4b shows the rates as a function of the ω_{SRR}. The solid gray line denotes the SRR-like widths we extrapolated from the data to obtain a reasonable estimate of the width of the uncoupled SRR. As for the phonon width, represented by the dashed gray line, we used the width of the phonon observed in the low-temperature spectra for a film without SRRs. One can see that when ω_{SRR} is small, ω_- has a lower damping than ω_+, showing its principle SRR character. Near the crossing, the lifetimes are equal, showing the mixed character. For large SRR frequency, ω_+, having the smallest damping, shows that now it has largely SRR character (and ω_- has largely phonon character). It is unclear as to why the ω_+ data for 1.1 THz are below the asymptote of 0.62 THz. We speculate that there are some overall changes to the profile of the electromagnetic fields as the SRR frequency is tuned.

CONCLUSIONS

In this work, we have demonstrated strong light−matter coupling between the α phonon mode of $(Bi_xSb_{1-x})_2Te_3$ and cavity resonances of planar THz range MMs. We have given spectroscopic evidence of strong coupling with a normalized

https://doi.org/10.1021/acsphotonics.3c01879
ACS Photonics 2024, 11, 2242−2246

coupling strength of $\eta \approx 0.09$. Consequently, we have observed the formation of THz phonon−polariton resonance emerging from the integration of MMs with TIs. Our findings hold promise for the advancement of TI-based electronics and plasmonic applications. We anticipate the possibility of transitioning into the regime of ultrastrong coupling for TI. Our work may facilitate the capture of photons for various applications, such as slow-light phenomena, quantum computing, and infrared light harvesting. By varying the MM resonance, we have demonstrated the ability to manipulate the mechanical properties of a material by tuning its electromagnetic environment. Via their coupling to phonons, this may be used to control magnetic and topological degrees of freedom.

■ ASSOCIATED CONTENT

Data Availability Statement

Source data are available for this paper. All other data that support the plots within this paper, and other findings of this study are available from the corresponding author upon reasonable request.

Supporting Information

The Supporting Information is available free of charge at https://pubs.acs.org/doi/10.1021/acsphotonics.3c01879.

Further details on the growth of the TI (bismuth antimony telluride), finite element simulation employed to derive the electromagnetic behavior of the split ring resonators, fabrication methods for creating the BST−SRR systems, spectroscopic technique applied to assess the fabricated devices, and methods used to interpret the optical response of the systems (PDF)

■ AUTHOR INFORMATION

Corresponding Author

N. P. Armitage − *William H. Miller III, Department of Physics and Astronomy, The Johns Hopkins University, Baltimore, Maryland 21218, United States*; Email: npa@jhu.edu, smm@jhu.edu

Authors

Sirak M. Mekonen − *William H. Miller III, Department of Physics and Astronomy, The Johns Hopkins University, Baltimore, Maryland 21218, United States;* orcid.org/0000-0003-4733-3243

Deepti Jain − *Department of Physics and Astronomy, Rutgers, The State University of New Jersey, Piscataway, New Jersey 08854, United States; Center for Quantum Materials Synthesis, Piscataway, New Jersey 08854, United States*

Seongshik Oh − *Department of Physics and Astronomy, Rutgers, The State University of New Jersey, Piscataway, New Jersey 08854, United States; Center for Quantum Materials Synthesis, Piscataway, New Jersey 08854, United States;* orcid.org/0000-0003-1681-516X

Complete contact information is available at: https://pubs.acs.org/10.1021/acsphotonics.3c01879

Author Contributions

SMM performed the simulation, fabrication, and TDTS measurements. DJ grew the thin films. SO and NPA supervised the project. SMM and NPA wrote the manuscript with input from other authors.

Notes

The authors declare no competing financial interest.

■ ACKNOWLEDGMENTS

Work at JHU was supported by NSF DMR-1905519 and an AGEP supplement. Work at Rutgers was supported by ARO-W911NF2010108 and MURI W911NF2020166. The work reported here was partially carried out in the Nanofabrication Facility at the University of Delaware (UDNF). We thank A. Jackson, K. Katsumi, and L.Y. Shi for helpful discussions.

■ REFERENCES

(1) Gramotnev, D. K.; Bozhevolnyi, S. I. Plasmonics beyond the diffraction limit. *Nat. Photonics* **2010**, *4*, 83−91.

(2) Shelton, D. J.; Brener, I.; Ginn, J. C.; Sinclair, M. B.; Peters, D. W.; Coffey, K. R.; Boreman, G. D. Strong coupling between nanoscale metamaterials and phonons. *Nano Lett.* **2011**, *11*, 2104−2108.

(3) Kim, H. S.; Ha, N. Y.; Park, J.-Y.; Lee, S.; Kim, D.-S.; Ahn, Y. H. Phonon-polaritons in lead halide perovskite film hybridized with THz metamaterials. *Nano Lett.* **2020**, *20*, 6690−6696.

(4) As' ham, K.; Al-Ani, I.; Lei, W.; Hattori, H. T.; Huang, L.; Miroshnichenko, A. Mie exciton-polariton in a perovskite metasurface. *Phys. Rev. Appl.* **2022**, *18*, 014079.

(5) Dintinger, J.; Klein, S.; Bustos, F.; Barnes, W. L.; Ebbesen, T. Strong coupling between surface plasmon-polaritons and organic molecules in subwavelength hole arrays. *Phys. Rev. B: Condens. Matter Mater. Phys.* **2005**, *71*, 035424.

(6) Ramezani, M.; Halpin, A.; Fernández-Domínguez, A. I.; Feist, J.; Rodriguez, S. R.-K.; Garcia-Vidal, F. J.; Gómez Rivas, J. Plasmon-exciton-polariton lasing. *Optica* **2017**, *4*, 31−37.

(7) In, C.; Sim, S.; Kim, B.; Bae, H.; Jung, H.; Jang, W.; Son, M.; Moon, J.; Salehi, M.; Seo, S. Y.; et al. Control over Electron−Phonon Interaction by Dirac Plasmon Engineering in the Bi_2Se_3 Topological Insulator. *Nano Lett.* **2018**, *18*, 734−739.

(8) Hasan, M. Z.; Kane, C. L. Colloquium: topological insulators. *Rev. Mod. Phys.* **2010**, *82*, 3045−3067.

(9) Ando, Y. Topological insulator materials. *J. Phys. Soc. Jpn.* **2013**, *82*, 102001.

(10) Wu, L.; Brahlek, M.; Valdés Aguilar, R.; Stier, A.; Morris, C.; Lubashevsky, Y.; Bilbro, L.; Bansal, N.; Oh, S.; Armitage, N. A sudden collapse in the transport lifetime across the topological phase transition in $(Bi_{1-x}\ In_x)_2Se_3$. *Nat. Phys.* **2013**, *9*, 410−414.

(11) Autore, M.; Di Pietro, P.; Di Gaspare, A.; D'Apuzzo, F.; Giorgianni, F.; Brahlek, M.; Koirala, N.; Oh, S.; Lupi, S. Terahertz plasmonic excitations in Bi_2Se_3 topological insulator. *J. Phys.: Condens. Matter* **2017**, *29*, 183002.

(12) Zhang, X.; Wang, J.; Zhang, S.-C. Topological insulators for high-performance terahertz to infrared applications. *Phys. Rev. B: Condens. Matter Mater. Phys.* **2010**, *82*, 245107.

(13) Chen, Y. L.; Analytis, J. G.; Chu, J.-H.; Liu, Z.; Mo, S.-K.; Qi, X.-L.; Zhang, H.; Lu, D.; Dai, X.; Fang, Z.; et al. others Experimental realization of a three-dimensional topological insulator, Bi_2Te_3. *Science* **2009**, *325*, 178−181.

(14) Dovzhenko, D.; Ryabchuk, S.; Rakovich, Y. P.; Nabiev, I. Light−matter interaction in the strong coupling regime: configurations, conditions, and applications. *Nanoscale* **2018**, *10*, 3589−3605.

(15) Benz, A.; Campione, S.; Klem, J. F.; Sinclair, M. B.; Brener, I. Control of strong light−matter coupling using the capacitance of metamaterial nanocavities. *Nano Lett.* **2015**, *15*, 1959−1966.

(16) Bakker, H.; Hunsche, S.; Kurz, H. Investigation of anharmonic lattice vibrations with coherent phonon polaritons. *Phys. Rev. B: Condens. Matter Mater. Phys.* **1994**, *50*, 914−920.

(17) Tanabe, T.; Suto, K.; Nishizawa, J.-i.; Saito, K.; Kimura, T. Frequency-tunable terahertz wave generation via excitation of phonon-polaritons in GaP. *J. Phys. D: Appl. Phys.* **2003**, *36*, 953−957.

(18) Kojima, S.; Tsumura, N.; Takeda, M. W.; Nishizawa, S. Far-infrared phonon-polariton dispersion probed by terahertz time-

domain spectroscopy. *Phys. Rev. B: Condens. Matter Mater. Phys.* **2003**, *67*, 035102.
(19) Jin, X.; Morandotti, R.; Lupi, S.; De Angelis, F.; Prato, M.; Toma, A.; Razzari, L.; Cerea, A.; Messina, G. C.; Rovere, A.; , et al. Modifying the Optical Phonon Response of Nanocrystals inside Terahertz Plasmonic Nanocavities. *European Quantum Electronics Conference*, 2019; p 6_3.
(20) Ohtani, K.; Meng, B.; Franckié, M.; Bosco, L.; Ndebeka-Bandou, C.; Beck, M.; Faist, J. An electrically pumped phonon-polariton laser. *Sci. Adv.* **2019**, *5*, 1632.
(21) Pons-Valencia, P.; Alfaro-Mozaz, F. J.; Wiecha, M. M.; Biolek, V.; Dolado, I.; Vélez, S.; Li, P.; Alonso-González, P.; Casanova, F.; Hueso, L. E.; et al. Launching of hyperbolic phonon-polaritons in h-BN slabs by resonant metal plasmonic antennas. *Nat. Commun.* **2019**, *10*, 3242.
(22) Liu, P. Q.; Luxmoore, I. J.; Mikhailov, S. A.; Savostianova, N. A.; Valmorra, F.; Faist, J.; Nash, G. R. Highly tunable hybrid metamaterials employing split-ring resonators strongly coupled to graphene surface plasmons. *Nat. Commun.* **2015**, *6*, 8969.
(23) Maier, S. A.; Andrews, S. R.; Martin-Moreno, L.; Garcia-Vidal, F. Terahertz surface plasmon-polariton propagation and focusing on periodically corrugated metal wires. *Phys. Rev. Lett.* **2006**, *97*, 176805.
(24) Liang, Y.; Yu, H.; Zhang, H. C.; Yang, C.; Cui, T. J. On-chip sub-terahertz surface plasmon polariton transmission lines in CMOS. *Sci. Rep.* **2015**, *5*, 14853.
(25) Latini, S.; Shin, D.; Sato, S. A.; Schäfer, C.; De Giovannini, U.; Hübener, H.; Rubio, A. The The ferroelectric photo ground state of $SrTiO_3$: Cavity materials engineeringerroelectric Photo Ground State of $SrTiO_3$: Cavity Materials Engineering. *Proc. Natl. Acad. Sci. U. S. A.* **2021**, *118*, No. e2105618118.
(26) Pendry, J. B.; Holden, A. J.; Robbins, D. J.; Stewart, W. Magnetism from conductors and enhanced nonlinear phenomena. *IEEE Trans. Microwave Theory Tech.* **1999**, *47*, 2075−2084.
(27) Zhang, Z.; Hirori, H.; Sekiguchi, F.; Shimazaki, A.; Iwasaki, Y.; Nakamura, T.; Wakamiya, A.; Kanemitsu, Y. Ultrastrong coupling between THz phonons and photons caused by an enhanced vacuum electric field. *Phys. Rev. Research* **2021**, *3*, L032021.
(28) Chen, H.-T.; Padilla, W. J.; Zide, J. M.; Gossard, A. C.; Taylor, A. J.; Averitt, R. D. Active terahertz metamaterial devices. *Nature* **2006**, *444*, 597−600.
(29) Kim, N.; In, S.; Lee, D.; Rhie, J.; Jeong, J.; Kim, D.-S.; Park, N. Colossal terahertz field enhancement using split-ring resonators with a sub-10 nm gap. *ACS Photonics* **2018**, *5*, 278−283.
(30) Yao, X.; Yi, H. T.; Jain, D.; Oh, S. Suppressing carrier density in $(Bi_xSb_{1-x})_2Te_3$ films using Cr_2O_3 interfacial layers. *J. Phys. D: Appl. Phys.* **2021**, *54*, 504007.
(31) Richter, W.; Becker, C. A Raman and far-infrared investigation of phonons in the rhombohedral V_2-VI_3 compounds Bi_2Te_3, Bi_2Se_3, Sb_2Te_3 and $Bi_2(Te_{1-x}\ Se_x)_3$ $(0 < x < 1)$,$(Bi_{1-y}\ Sb_y)_2\ Te_3$ $(0 < y < 1)$. *Phys. Status Solidi b* **1977**, *84*, 619−628.
(32) Pal, S.; Nongt, H.; Markmann, S.; Kukharchyk, N.; Valentin, S.; Scholz, S.; Ludwig, A.; Bock, C.; Kunze, U.; Wieck, A.; et al. Strong coupling of intersubband resonance in a single triangular well to a THz metamaterial. *40th International Conference on Infrared, Millimeter, and Terahertz waves (IRMMW-THz)*, 2015; pp 1−2.
(33) Novotny, L. Strong coupling, energy splitting, and level crossings: A classical perspective. *Am. J. Phys.* **2010**, *78*, 1199−1202.

https://doi.org/10.1021/acsphotonics.3c01879
ACS Photonics 2024, 11, 2242−2246